Journal of Alloys and Compounds 509 (2011) 2473–2477

Contents lists available at ScienceDirect

Journal of Alloys and Compounds

journal homepage: www.elsevier.com/locate/jallcom

Enhancement of the magnetic properties of Ni–Cu–Zn ferrites by the non-magnetic Al^{3+}-ions substitution

M.M. Eltabey*, K.M. El-Shokrofy, S.A. Gharbia

Basic Engineering Science Department, Faculty of Engineering, Menoufiya University, Shebin El-Kom, Egypt

ARTICLE INFO

Article history:
Received 1 January 2010
Received in revised form 6 November 2010
Accepted 10 November 2010
Available online 26 November 2010

Keywords:
Ni–Cu–Zn ferrites
Magnetization
Initial permeability

ABSTRACT

The effect of Al-substitution on the physical, magnetic and electrical properties of Ni–Cu–Zn ferrite of chemical formula $Ni_{0.4}Cu_{0.2}Zn_{0.4}Al_xFe_{2-x}O_4$ ($x = 0$ to $x = 0.15$ with step = 0.025) which prepared by conventional ceramic method has been studied. X-ray patterns indicated the presence of a single spinel phase. Analysis of IR-spectrum indicated the occupation of Al-ions the octahedral site in ferrite lattice. SEM micrographs showed that the average grain size D decreased with increasing Al-content. The magnetization is measured using VSM at room temperature. The initial permeability is measured, on toroidal samples used as transformer cores, as a function of temperature at constant frequency of 10 kHz and Curie temperature (T_c) is determined. It was found that Al-ion substitute improved the magnetization as well as the initial permeability with no considerable effect for it on the value of T_c. The dc resistivity is also increased with increasing Al-concentration. Such results are promising ones for the high frequency applications.

1. Introduction

Ferrites are very important in technological applications as inductor cores because they have high resistivity compared to metallic materials. The magnetic properties of ferrites such as the permeability, magnetization and coercive field are affected by the type of the substituted ion, microstructure and the porosity [1]. The miniaturization trend of electronic devices results in the rapid development of surface mount devices (SMD) [2,3]. As one of the most important SMD, multilayer chip inductors (MLCI) become more and more miniaturized and integrated [4]. Ni–Cu–Zn ferrite is one of the soft magnetic materials which is used for MLCI applications because of their relatively low sintering temperature, high permeability in the R-F frequency region and high electrical resistivity [5,6]. The effect of substituting trivalent ions for iron in ferrites has been investigated [7–9]. The effect of Al-substitution on the magnetic and electrical properties of different ferrites was studied by many authors [10–14]. Unfortunately, they reported that, due to the substitution, there was a decrease in the values of saturation magnetization M_S, initial permeability μ_i, Curie temperature, remanence ratio R, and coercive field whereas the anisotropy field and electrical conductivity were increased. In previous work, [15,16], a significant effect due to the Al-substitution on the magnetic and electrical properties were reported in the $Mn_{0.5}Ni_{0.1}Zn_{0.4}Al_xFe_{2-x}O_4$ ferrite system ($0 \le x \le 0.15$ in steps of 0.025). Many studies were carried out on the Ni–Cu–Zn ferrite systems keeping the Cu-concentration at 0.2 [17–21]. Furthermore, Ref. [22] reported that, for Cu-substituted Ni–Zn ferrite, the bulk density, initial permeability and dc electrical resistivity increased with optimum copper concentration of $x = 0.2$. In the present study, keeping the Zn-concentration equal to 0.4 which corresponding to the maximum magnetization in Cu/Ni–Zn ferrites [23], the effect of Al^{3+}-ions substitution on the physical, magnetic and electrical properties of $Ni_{0.4}Cu_{0.2}Zn_{0.4}Al_xFe_{2-x}O_4$ ferrites will be studied.

2. Experimental procedure

Samples with the chemical formula $Ni_{0.4}Cu_{0.2}Zn_{0.4}Al_xFe_{2-x}O_4$ ($x = 0$ to $x = 0.15$ with step = 0.025) were prepared by using standard ceramic technique. High purity oxides, 99.9% of NiO, CuO, ZnO, Al_2O_3 and Fe_2O_3 were mixed together according to their molecular weights. The mixture of each sample was ground to a very fine powder and then presintered at 900 °C for 12 h in one cycle. The presintered mixture was ground again and pressed at room temperature into discs and toroids. They were finally sintered at 1200 °C for 5 h and then slowly cooled at room temperature. X-ray diffraction (XRD) patterns were formed using diffractometer of type x'pert Graphics identify with CuKα radiation. The porosity percentage (P%) was calculated for all samples according to the relation $P\% = 100[1 - (d/d_x)]$ %, where d_x is the theoretical X-ray density of samples which calculated using the formula $d_x = 8M/Na^3$ (M is the molecular weight, N is Avogadro's number and a is the lattice parameter) and d is the density of each composition measured in water using Archimedes principle. FTIR spectra were carried out (using Perkin Elmer spectro-photometer) in the range from 150–650 cm^{-1}. The grain micrographs were obtained by low vacuum scanning electron microscope (SEM type JEOL JSM5600). The magnetization M (emu/g) is measured at room temperature in the magnetizing field H (Oe) ranged from zero to 6000 Oe using the LDJ vibrating sample magnetometer (VSM) model 9600. The initial permeability (μ_i) was measured as a function of temperature at constant frequency

* Corresponding author. Tel.: +20 12 3778714; fax: +20 48 2235695.
E-mail address: mohamed.eltabey@yahoo.com (M.M. Eltabey).

0925-8388/$ – see front matter © 2010 Elsevier B.V. All rights reserved.
doi:10.1016/j.jallcom.2010.11.056

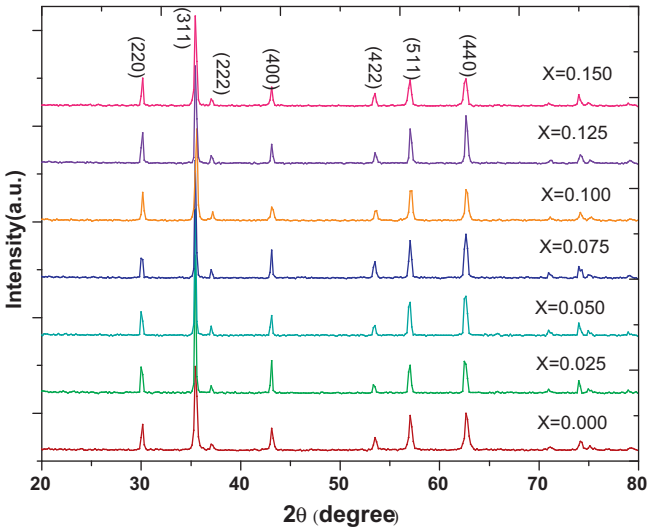

Fig. 1. X-ray diffraction pattern of $Ni_{0.4}Cu_{0.2}Zn_{0.4}Al_xFe_{2-x}O_4$.

(f = 10 kHz) and low magnetizing current of I_p = 10 mA. The value of μ_i was calculated using poltinnikov's formula [24]. which is given by $V_s = K\mu_i$, $K = 0.4\pi N_p N_s I_p A\omega/L$ where V_s is the induced voltage in secondary coil, N_p and N_s are the number of turns of primary and secondary coils, respectively ($N_p = N_s$ = 20 turns). A is the cross-sectional area of the sample, ω is the angular frequency ($\omega = 2\pi f$) and L is the average path of magnetic flux ($L = 2\pi r_m$) where r_m is the mean radius of toroid. The dc resistivity was measured using tablet shape samples by the two-probes method with In–Hg contacts.

3. Results and discussion

3.1. Physical properties

3.1.1. X-ray analysis

The XRD patterns, in Fig. 1, indicate that all investigated samples are formed in cubic single spinel phase. The values of d-spacing are calculated according to Bragg's law and hence the average lattice parameter a (Å) is calculated. The variation of a (Å) with the Al-concentration is plotted in Fig. 2. It is clear that as Al-concentration increases the lattice parameter decreases almost linearly obeying vegard's law. Similar behavior was observed in Al-substituted Mn–Zn [25,26], Ni–Zn [27] and Mn–Ni–Zn ferrites [15]. The decrease in lattice parameter with increasing Al-concentration could be explained on the basis of the ionic radii due to the replacement of ions with larger ionic radius of Fe^{3+} (0.64 Å) by the smaller one Al^{3+} (0.51 Å).

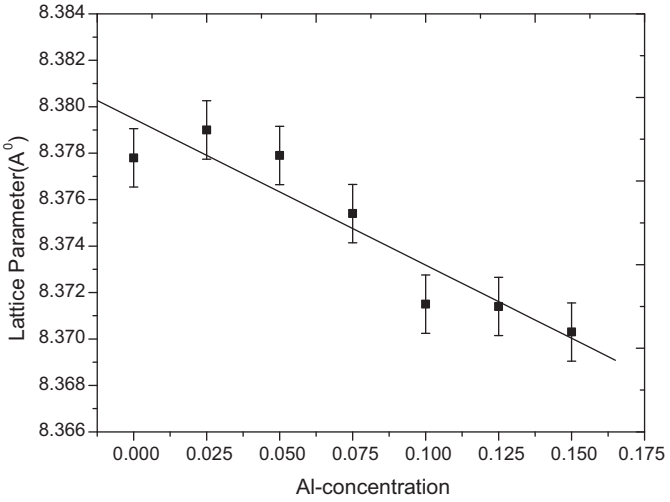

Fig. 2. Variation of lattice parameter a (Å) with Al-concentration.

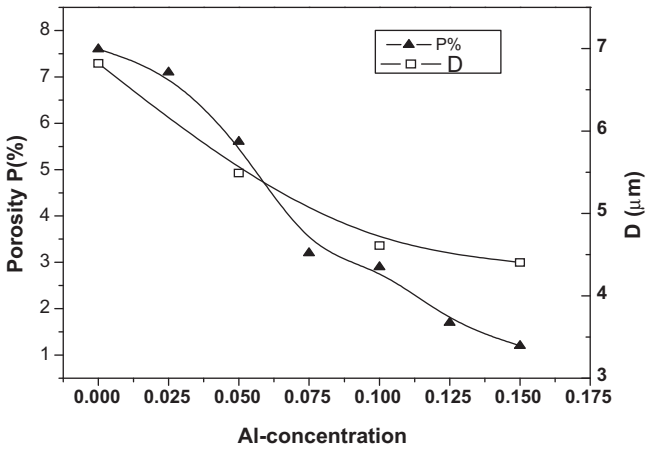

Fig. 3. The variations of porosity (P%) and the grain size (D) with Al-concentration.

3.1.2. Porosity and grain size

The variations of porosity (P%) and the grain size with Al-concentration (x) are shown in Fig. 3. It is obvious that, as Al-concentration increases the porosity decreases. This behavior could be explained as follows: it is well known that the porosity of ceramic samples results from two sources intragranular porosity (P_{intra}) and intergranular porosity (P_{inter}) [28]. Thus, the total porosity (P%) could be written as the sum of two types i.e.

$$P\% = P_{intra} + P_{inter} \quad (1)$$

Furthermore, it was reported that the intergranular porosity (P_{inter}) is directly proportional to the grain size [29,30]. Fig. 4 shows the SEM micrographs to four selected samples. The average grain size (D) of each sample was determined using main linear intercept method by drawing random lines on the obtained photographs and counting the number of grain boundaries [31]. The average grain size (μm) was calculated by dividing the length of the straight line over the number of grain boundaries. It is found that, see Fig. 3, as Al-concentration increases the average grain size decreases. From this behavior one can observe that, the behaviors of D, P_{inter} and P% are the same. Thus according to Eq. (1), one could be conclude that the total porosity P (%) for these samples results mainly from the intergranular porosity (P_{inter}).

3.1.3. IR spectra analysis

The study of far-infrared spectrum is an important tool to get information about the position of ions in the crystal through the vibrational modes [32]. According to the group theory, the normal and inverse cubic spinel should have four IR bands representing the four fundamentals (ν_1, ν_2, ν_3 and ν_4) [33]. It has been reported that, the first three IR fundamental bands are due to tetrahedral and octahedral complexes, while the fourth one is due to the lattice vibrations [32].

Fig. 5 shows the IR spectra of four selected samples with x = 0.0, 0.05, 0.1 and 0.15. The positions of their bands are reported in Table 1, where the high frequency bands ν_1 (about 570) and ν_2 (393–397) are attributed to the vibrations of iron ions in both tetrahedral and octahedral positions respectively. The third vibrational frequency band ν_3 (339–285) is associated with the divalent octahedral metal ions and oxygen complexes. Finally, the lattice vibrational frequency band, ν_4, is in the range (208–270) cm^{-1} [34]. It is obvious from the table that, as the Al-concentration (x) increases ν_1 almost constant while ν_2 and ν_3 increase. These results reveal that the radius of octahedral site r_B decrease with Al-content

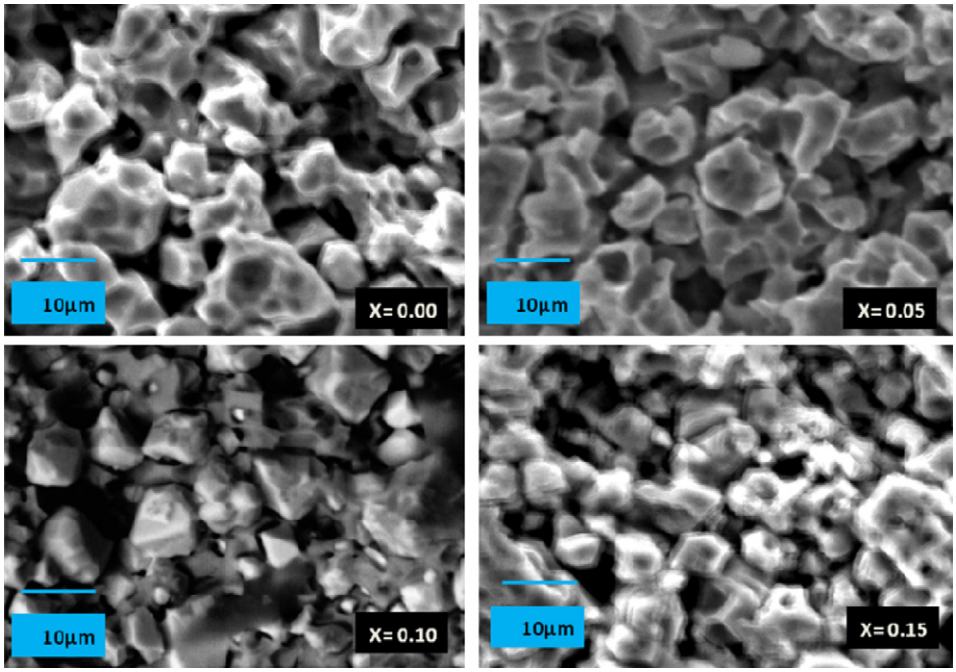

Fig. 4. SEM micrographs of $Ni_{0.4}Cu_{0.2}Zn_{0.4}Al_xFe_{2-x}O_4$ with $x = 0.0$, 0.05, 0.10 and 0.15.

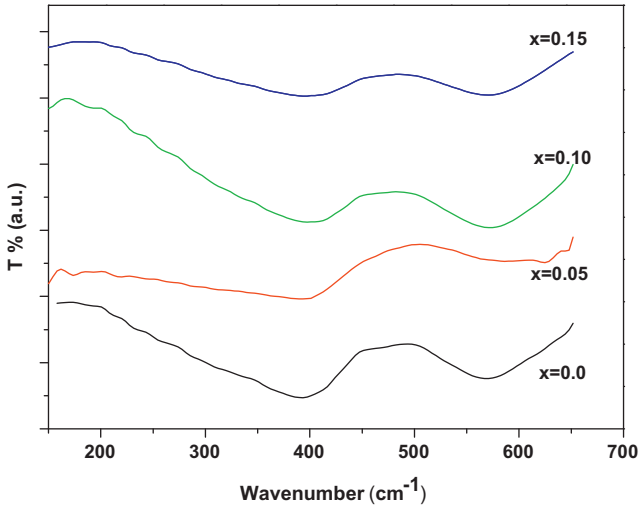

Fig. 5. Infrared spectra of $Ni_{0.4}Cu_{0.2}Zn_{0.4}Al_xFe_{2-x}O_4$ with $x = 0.0$, 0.05, 0.1, and 0.15.

where the band frequency is inversely proportional to the bond length [25]. The shift of the lattice vibration band ν_4 to the higher frequency could be attributed to the difference in masses between substituted and displaced ions. In our composition, we replace Fe^{3+}-ions by Al^{3+}, which has smaller mass, thus the total mass of lattice decreases leading to increase the frequency of ν_4 band ($\nu\alpha\sqrt{1/m}$).

Therefore, in the light of the above discussion of the spectra, one could be conclude that Al^{3+}-ions completely occupy B-site. Also, it is well known that Zn^{2+}-ions prefer to occupy A-site, where Cu^{2+}-ions prefer to occupy B-site. Then, the following cation distribution is assumed.

$$(Zn_{0.4}Fe_{0.6})[Ni_{0.4}Cu_{0.2}Al_xFe_{1.4-x}]O_4 \quad (2)$$

where the brackets () and [] denote to A- and B-sites, respectively.

Table 1
Change of wave number (cm^{-1}) of the IR observed bands with Al-content.

Al-conc.	Tetra.	Octahedral bands			Lattice vibration		
(x)	ν_1	ν_2	ν_3		ν_4		
0	570	393	339	285	254	231	208
0.05	572	396	352	286	259	234	209
0.1	571	397	360	289	264	238	208
0.15	570	395	362	289	270	235	208

3.2. Magnetic properties

3.2.1. Magnetization

The variation of magnetization M (emu/g) with applied magnetic field H(Oe) for all investigated samples at room temperature is shown in Fig. 6. As a normal behavior, the magnetization increases with increasing applied magnetic field and attain its saturation value for higher fields. The dependence of saturation magnetization (M_s) on Al-concentration is shown in Fig. 7. It is clear that, as Al-concentration increases M_s increases up to its maximum value at

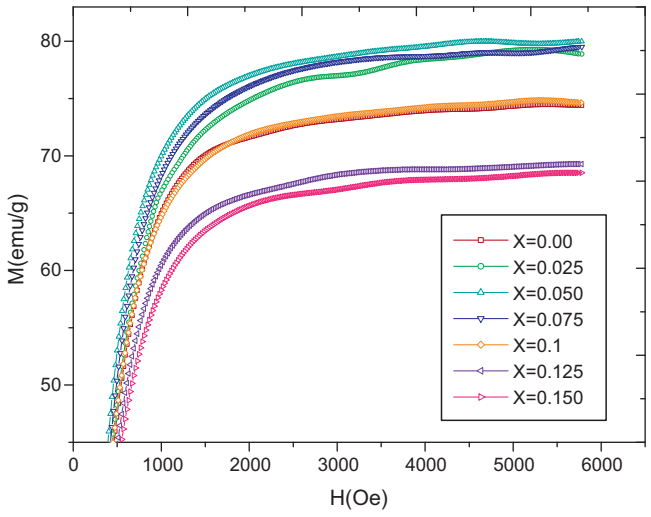

Fig. 6. Variation of magnetization M (emu/g) with H (Oe) for $Ni_{0.4}Cu_{0.2}Zn_{0.4}Al_xFe_{2-x}O_4$.

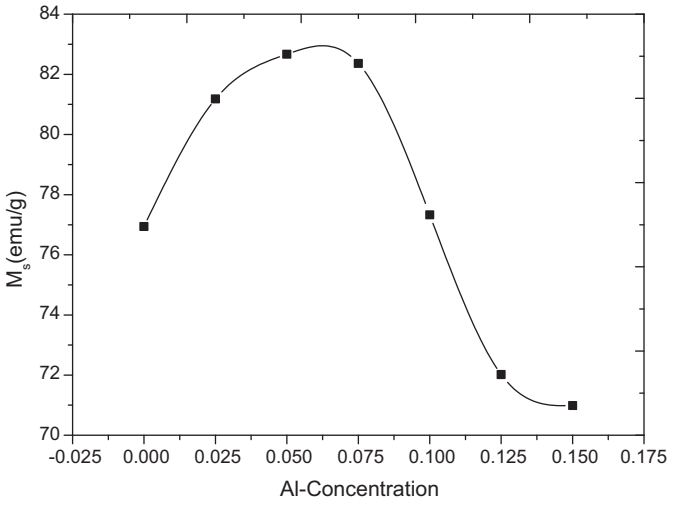

Fig. 7. Variation of saturation magnetization M_s (emu/g) with Al-concentration.

$x = 0.05$, with percentage increase $\Delta M_s\% = 6.9\%$, and then decreases. This could be explained as following: it is known that, for Ni–Zn and Cu–Zn ferrites there is a canting angle, Yafet-Kittel angle (α_{YK}), between moments in B-site at Zn concentration = 0.4. Such a canting angle is due to the negative B–B interaction [23,35]. Thus, the total magnetization could be expressed as:

$$M = M_B \cos \alpha_{YK} - M_A \quad (3)$$

where M_A and M_B are the magnetic moments of A- and B-sites, respectively [36]. According to Eq. (2), M_A and M_B could be written using the values of magnetic moments for Ni^{2+} ($2\mu_B$), Cu^{2+} ($1\mu_B$), Zn^{2+} ($0\mu_B$), Al^{3+} ($0\mu_B$) and Fe^{3+} ($5\mu_B$) as:

$$M_A = (0.4 * 0 + 0.6 * 5)\mu_B,$$

$$M_B = (0.4 * 2 + 0.2 * 1 + x * 0 + (1.4 - x) * 5)\mu_B$$

Thus the total magnetic moment in Eq. (3) is given by,

$$M = \mu_B(8 - 5x)\cos \alpha_{YK} - 3\mu_B \quad (4)$$

In view of Eq. (4) and according to the value of x, the increase of M_s up to $x = 0.05$ with increasing Al-concentration could be attributed to the increase of $\cos \alpha_{YK}$ i.e. decreasing of α_{YK} due to the decrease of the negative B–B interaction leading to enhancing the parallelism of moments in B-site. For $x > 0.05$, i.e. further replacement of the magnetic Fe^{3+}-ions by non magnetic Al^{3+}-ions in B-site leads to a decrease of the magnetization of B-site and hence the total magnetization should decrease.

3.2.2. Initial permeability and Curie temperature

Fig. 8 shows the variation of the initial permeability (μ_i) with temperature T (K) for all samples. It is found that the curves are typical of multi domain grains showing a sudden drop in μ_i at the Curie temperature (T_c). It is determined by drawing a tangent for the curve at the rapid decrease of μ_i. The intersection of the tangent with T-axis determines T_c. It was reported that the sharp decrease of μ_i with temperature at T_c reflects the homogeneity of the sample which can be expressed as the slope of the linear part ($\Delta\mu_i/\Delta T$) at T_c [37,38]. It is known that the increase of the grain size occurs at the expense of the grain boundaries i.e. samples with larger grain size expected to be more homogenous. One can note that, as Al-content increases the slope of the linear part decreases due to the decrease of the grain size which confirms the later statement. The dependence of both the initial permeability μ_i at room temperature and T_c on the Al-concentration are shown in Fig. 9. It is clear that, as

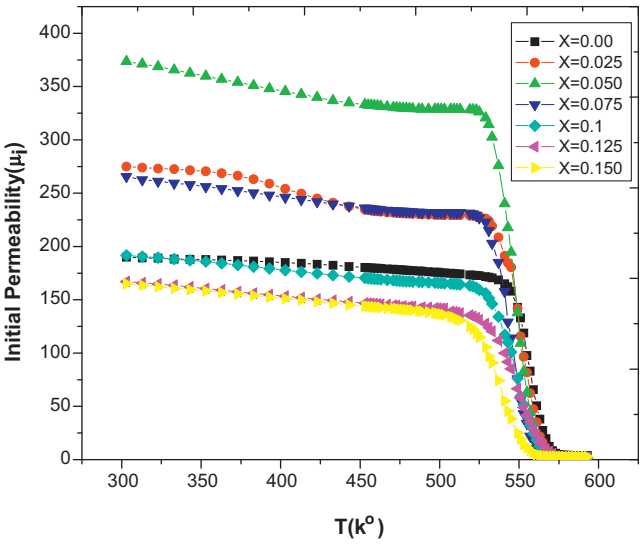

Fig. 8. Variation of the initial permeability (μ_i) with temperature T (K) of $Ni_{0.4}Cu_{0.2}Zn_{0.4}Al_xFe_{2-x}O_4$.

Al-concentration increases μ_i increases up to its maximum value at $x = 0.05$, with percentage increase $\Delta\mu_i\% \approx 96\%$, and then decreases. The similarity in behavior of μ_i, D and M_s with Al-concentration could be understood in view of the approximate equation for initial permeability [1,15,37].

$$\mu_i \cong \left(\frac{M_s^2 D}{\sqrt{K_1}}\right) \quad (5)$$

where M_s, K_1 and D are saturation magnetization, the anisotropy constant and the average grain size respectively. It is known that the anisotropy field in ferrites results from the presence of Fe^{2+}-ions which formed during the sintering process [39,40]. Therefore, the replacement of Fe^{3+}-ions by Al^{3+}-ions leads to decrease the anisotropy constant, with increasing the Al-concentration, due to the relative reduction in Fe^{2+}-ion concentration. The increase of μ_i with Al-concentration up to $x = 0.05$ is attributed to the increase of M_s and the decrease of K_1.While in the range of $x > 0.05$, it is clear that the value of μ_i decreases with increasing Al-concentration. This means that the decrease of both M_s and D with Al-concentration in that range have the dominant effect.

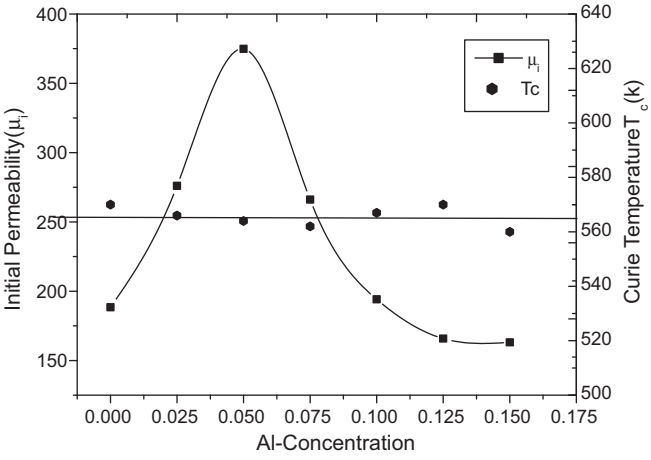

Fig. 9. Variation of initial permeability (μ_i) at room temperature and Curie temperature (T_c) with Al-concentration.

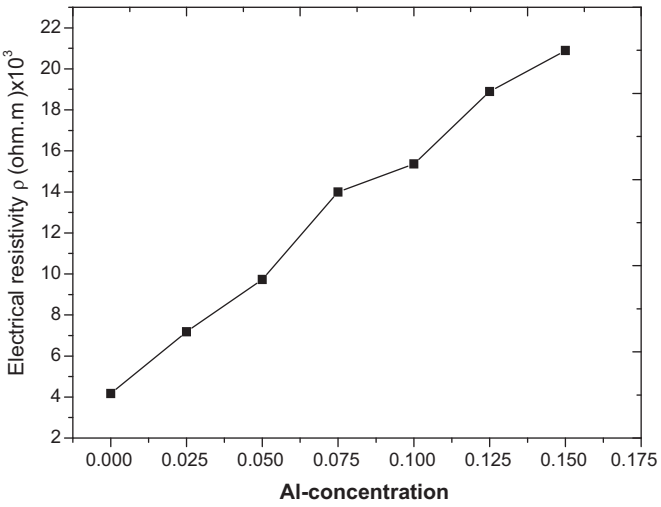

Fig. 10. The dependence of the electrical resistivity (ρ) at room temperature on Al-concentration.

Fig. 9 shows also that there is no considerable change in Curie temperature with increasing Al-concentration. This constancy could be explained in the light of pair model. Where, the main factor that affects the value of T_c is the A–B interaction [23]. The constancy of T_c could be attributed to a competition between two factors: first, the decrease in the distance between the moments of A and B sites as noted from lattice parameter leads to increase of A–B interaction and hence T_c has to increase. On the other hand, due to the replacement of the magnetic Fe^{3+}-ions by the non magnetic Al^{3+}-one, the A–B interaction have to decrease leading to decrease T_c.

3.3. Electrical resistivity

The dependence of dc electrical resistivity (ρ) at room temperature on Al-concentration is shown in Fig. 10. It is clear that, as Al-concentration increases the resistivity increases. Similar behavior was reported for Al-substituted ferrites [41–43]. This behavior of ρ could be attributed to the decrease of Fe^{2+} and Fe^{3+}-ions concentrations with increasing the Al-concentration. This leads to limit the hopping probability between Fe^{3+} and Fe^{2+}-ions.

4. Conclusion

The lattice parameter decreased as well as both porosity and average grain size with increasing Al^{3+}-ion substitution in Ni–Cu–Zn ferrites. IR-spectrum indicated the occupation of Al-ions the octahedral site. Al-ion substitution in that ferrite improved the saturation magnetization, the initial permeability and dc resistivity whereas there was no considerable effect in the value of Curie temperature due to the Al-substitution.

References

[1] G.C. Jain, B.K. Das, R.S. Khanduja, S.C. Gupta, J. Mater. Sci. 11 (1976) 1335–1338.
[2] I.Z. Rahman, T.T. Ahmed, J. Magn. Magn. Mater. 290–291 (2005) 1576.
[3] C.W. Kim, J.G. Koh, J. Magn. Magn. Mater. 257 (2003) 355.
[4] B. Li, Z.X. Yue, X.W. Qi, J. Zhou, Z.L. Gui, L.T. Li, Mater. Sci. Eng. B 99 (2003) 252.
[5] K.O. Low, F.R. Sale, J. Magn. Magn. Mater. 246 (2002) 30–35.
[6] H.I. Hsiang, W.C. Liao, Y.J. Wang, Y.F. Cheng, J. Eur. Ceram. Soc. 24 (2004) 2015–2021.
[7] K.P. Belove, L.A. Antoshina, A.S. Moreosyan, Sov. Phys. – Solid State 25 (1993) 1609.
[8] M.A. Ahmed, Tawfik, El-Nimr, El-Hasab, J. Mater. Sci. 10 (1991) 549.
[9] A.M. Samy, H.M. El-Sayed, A.A. Sattar, J. Phys. Stat. Sol. (A) 200 (2) (2003) 401–406.
[10] A.G. Bhosale, B.K. Chougule, J. Mater. Chem. Phys. 97 (2006) 273–276.
[11] G.J. Baldha, K.G. Saija, K.B. Modi, H.H. Joshi, R.G. Kulkarni, J. Mater. Lett. 53 (2002) 233–237.
[12] Y.-P. Fu, S. Tsao, C.-T. Hu, Y.-D. Yao, J. Alloy Compd. 395 (2005) 272–276.
[13] A.M. Sankpal, S.S. Suryawanshi, S.V. Kakatkar, G.G. Tengshe, R.S. Patil, N.D. Chaudhari, S.R. Sawant, J. Magn. Magn. Mater. 186 (1998) 349–356.
[14] U.V. Chhaya, B.S. Trivedi, R.G. Kulkarni, J. Phys. B 262 (1999) 5–12.
[15] A.A. Sattar, H.M. El-Sayed, K.M. El-Shokrofy, M.M. El-Tabey, J. Appl. Sci. 5 (1) (2005) 162–168.
[16] A.A. Sattar, H.M. El-Sayed, M.M. El-Tabey, J. Mater. Sci. 40 (18) (2005) 4873–4879.
[17] Z. Yue, J. Zhou, L. Li, Z. Gui, J. Magn. Magn. Mater. 233 (2001) 224–229.
[18] M.A. Gabal, J. Magn. Magn. Mater. 321 (2009) 3144–3148.
[19] P.K. Roy, J. Bera, J. Magn. Magn. Mater. 321 (2009) 247–251.
[20] H. Jun, Y. Mi, J. Zhejiang Univ. Sci. 6B (6) (2005) 580–583.
[21] H. Su, H. Zhang, X. Tang, Zhiyong, Y. Jing, J. Mater. Sci. Eng. B 162 (2009) 22–25.
[22] J.J. Shrotri, S.D. Kulkarni, C.E. Deshpande, A. Mitra, S.R. Sainkar, P.S. Anil Kumar, S.K. Date, J. Mater. Chem. Phys. 59 (1999) 1–5.
[23] S. ChikaZumi, S. Charap, Physics of Magnetism, John Wiley and Sons, Inc., New York, London, Sydney, 1964, p. 93.
[24] S.S. Poltinnikov, H. Turkevic, Sov. Phys. – Solid State 8 (1966) 1144.
[25] Chandrase Karan, G.S. Selvandan, K. Manivannane, J. Mater. Sci.: Mater. Electron. 15 (2004) 15–18.
[26] S.V. Kakatkar, S.S. Kakatkar, R.S. Patil, P.K. Maskar, A.M. Sankapal, S.S. Suryawanshi, N.D. Chaudhari, S.R. Sawant, J. Magn. Mater. 159 (1996) 361–366.
[27] P. Chandra, J. Mater. Sci. Lett. 6 (1987) 651–652.
[28] W.D. Kigery, H.K. Bowen, D.R. Uhlmann, Introduction of Ceramics, John Wiley and Sons, New York, London, and P.P., 1975, p. 458.
[29] Rezlescu, N.E. Rezlescu, C. Pasnicu, M.L. Graus, J. Phys. Condens. Matter 6 (1994) 5707.
[30] R.G. Kulkarni, V.U. Patial, J. Mater. Sci. 17 (1982) 843–848.
[31] P.J. Van der Zaag, J.J. Ruigrok, A. Noordermeer, Van Delden, J. Appl. Phys. 74 (6) (1993) 4085.
[32] K. Mohan, Venudhar, J. Mater. Sci. Lett. 18 (1999) 205.
[33] Ravinder, J. Mater. Lett. 40 (1999) 205.
[34] M.A. Ahmed, E. Ateia, S.I. El-Dek, J. Vib. Spectrosc. 30 (2002) 61.
[35] S.S. Suryawanshi, V. Deshpand, S.R. Sawant, J. Mater. Chem. Phys. 59 (1999) 199–203.
[36] E. Cedillo, J. Ocampo, V. Rioera, J. Phys. E: Sci. Instrum. 13 (1980) 383.
[37] A.A. Sattar, A.H. Wafik, K.M. El-Shokrofy, M.M. El-Tabey, Phys. Stat. Sol. (A) 171 (1999) 563.
[38] A.A. Sattar, A.M. Samy, J. Mater. Sci. 37 (2002) 449.
[39] S. ChikaZumi, S. Charap, Physics of Magnetism, John Wiley and Sons, Inc., New York, London, Sydney, 1964, p. 153.
[40] E.W. Gorter, Philips Res. Rep. 9 (1954) 295.
[41] A.M. Abo El Ata, S.M. Attia, T.M. Meaz, J. Solid State Sci. 6 (2004) 61.
[42] Chandra Prakash, J. Mater. Sci. Lett. 6 (1987) 651.
[43] T.O. Mason, H.K. Bowen, J. Am. Ceram. Soc. 64 (1981) 237.